Effect of calcium lignosulphonate on the particulate processes during hydrogen reduction of nickel ammine sulphate solutions

R.A. Iloy[a], F. Ntuli[a,*]

[a] Department of Chemical Engineering, Faculty of Engineering and the Built Environment, University of Johannesburg, P.O. Box 524, Auckland Park 2006, Johannesburg, South Africa

Abstract

The use of additives in the precipitation of nickel with hydrogen is known to influence the particulate processes and by extension the powder properties such as morphology, microstructure and particle size distribution. Controlling these properties is crucial for some downstream processes. The present study assesses the effect of calcium lignosulphonate on the particulate processes taking place during the reduction of nickel ammine sulphate solutions by hydrogen gas. Reactions were carried out in an autoclave operated at 28 bar and 180°C under stirring conditions of 850 rpm. Particulate processes were studied by analysing the particle size distribution and the corresponding normalized moments. These were further validated by scanning electron microscopy and nitrogen physisorption analyses. The powder phase identification and purity were determined by means of X-ray diffraction and X-ray fluorescence respectively. Calcium lignosulphonate acted as a reduction catalyst, growth promoter and by extension agglomerating agent. At 2, 5 and 7 mg/L of calcium lignosulphonate, the system was found to be dominated by breakage while agglomeration was more pronounced at 10 mg/L, as validated by scanning electron micrographs. Furthermore the use of calcium lignosulphonate resulted in the increase of the reduction rate, indicating that this additive acted as a growth promoter.

Keywords: Nickel reduction; Calcium lignosulphonate; precipitation; crystallization

*Corresponding author. Tel..: +27115596003

E-mail address: fntuli@uj.ac.za

1. Introduction

Hydrogen reduction is the most efficient and widely used method to precipitate metal powders from solutions (Meddings and Mackiw, 1965; Agrawal et al., 2006). Approximately 240,000 tons of nickel alone is produced this way per year worldwide. Commercial operations using this technology include, among others, Impala Platinum (South Africa), Sherritt (Canada) and Murrin Murrin (Australia) (Crundwell et al., 2011). Hydrogen reduction is a process whereby an ammoniacal aqueous metal salt solution is subjected to hydrogen at elevated pressures and temperatures in mechanically agitated autoclaves. Under these conditions, the dissolved metal ions undergo reduction and precipitate as metallic powders. The possibility of precipitating metals from solutions using gases as reducing agents was first established by Beketov in the 1860's (Agrawal et al., 2006). The earliest interest was in the reduction of copper sulphate solutions using sulphur dioxide and carbon monoxide as reducing agents. The use of hydrogen as a reducing agent was investigated during the period 1909 – 1931 in the precipitation of metals from their aqueous and organic solutions. In these investigations, reactions were done at elevated hydrogen pressure and temperature in sealed and unagitated tubes. As a result, products were contaminated with stable oxides and basic salts (Evans, 1968). The commercialization of the hydrogen reduction process was made possible by Chemical Construction Corporation in the 1950's after an extensive research and developmental work (Habashi, 1999; Osseo-Asare, 2003).

Since the commercialization of the gaseous reduction technology, additives or addition agents have been identified as playing a major role in the operation of the process. In fact, in this process the precipitated metals have the tendency to agglomerate and plate out on the impeller of the agitator and the walls of the reaction vessel. Addition agents assist in lessening the surface activity of the reduced metal particles and therefore inhibit plating and agglomeration. Furthermore, they accelerate the reaction, making it possible to achieve reduction at shorter periods of time. They also help in controlling the physical characteristics of the obtained powder such as morphology, size and bulk density which constitute important parameters for downstream processes (Chou et al., 1976; Saarinen et al., 1998; Agrawal et al., 2006; Luidold and Antrekowitsch, 2007; Naboychenko et al., 2009). As an example, in fuel cell technologies, the porosity of materials used to construct the electrodes is a critical parameter amongst others. These elements altogether contribute in making the gaseous reduction technology commercially viable. However, commercial additives are quite expensive and in most cases their function and mechanism of action are not well understood, with most of them being

employed on a trial and error basis (Bodoza et al., 2013). Since additives are normally one of the major operational costs in commercial operations, developing an understanding of their mechanism of action will enable their optimum use in industry.

The aim of this study was to establish the mechanisms involved in powder formation in the presence of calcium lignosulphonate in high-pressure hydrogen reduction of ammoniacal nickel sulphate solutions. This additive is of commercial importance in the production of nickel powders and has not been studied extensively. To the best of our knowledge, the only published data in literature are those of Sherritt Research and Development Division by Kunda and co-workers (Kunda et al., 1965; Kunda and Evans, 1968). In these studies, calcium lignosulphonate along with other additives were investigated at fixed concentration at the initial densification, and details on the effect of some individual additives were not reported. This paper intends to address these limitations since additives are known to influence the precipitation mechanism differently with varying concentrations and number of densifications.

2. Materials and methods

2.1. Chemicals

All the chemicals used in this set of experiments were of analytical grade provided by Sigma-Aldrich and Rochelle Chemicals except for nickel powder which was supplied by Impala Platinum. Sulphuric acid (98 wt.%), used for titration purposes and free ammonia to nickel ratio adjustments, was supplied by Rochelle Chemicals along with nitric acid (55 wt.%), anhydrous sodium carbonate, ammonium sulphate and ammonia solution (25 wt.%). Nickel sulphate hexahydrate (99 wt.%) and methyl orange on the other hand were supplied by Sigma-Aldrich. Nitrogen and hydrogen with purity greater than 99.99% were used for purging and reduction respectively. Both gases were supplied by African Oxygen Limited (Afrox).

2.2. Apparatus

Experiments were conducted in a 750 mL laboratory scale stainless steel (SS 316) autoclave with a maximum allowable working pressure of 100 bar that could be operated at temperatures of up to 250°C. The autoclave height and internal diameter were 193 mm and 75 mm respectively. Agitation was achieved by a double pitched six-bladed turbine impellers (diameter 35 mm) with a spacing of 60 mm mounted on a shaft driven by a 0.18 kW electric motor. The lower impeller had an off-bottom clearance of 10 mm. Other internal parts of the autoclave included a serpentine cooling coil, a thermowell housing a thermocouple and a dip

tube through which gases were admitted. Heating was achieved by means of an electric heating mantle (1.25 kW) around the vessel and controlled by means of a control panel with PID temperature controller. The same control panel also allowed for the motor speed to be adjusted in terms of number of revolutions per minute (rpm) which could be varied from 50 to 1450 rpm. Pressure readings were made possible by a bourdon type pressure gauge with a range of 0 – 100 bar.

2.3. Reduction procedure

The pressure reactor was first loaded with 30 g of nickel powder as seeding material, a predetermined amount of ethylene maleic anhydride and 450 mL of an aqueous solution of nickel sulphate, ammonium sulphate and ammonia. This solution contained 10.51 g/L Ni^{2+} with molar ratios of $(NH_4)_2SO_4/Ni^{2+}$ and NH_3/Ni^{2+} of 2.1 and between 2.0 – 2.1 respectively. The preparation of the synthetic solution has been previously reported (Ntuli and Lewis, 2007). On the controller, the temperature and agitation speed were then set to 180°C and 850 rpm respectively. In order to expel oxygen from the system, the reactor was successively flushed with nitrogen and hydrogen gases at 10 bar. As soon as the reactor temperature reached 170°C, hydrogen was introduced to the reaction vessel, bringing the system pressure to 28 bar. The hydrogen supply to the system was kept constant throughout reduction. At the end of reduction, agitation and heating were stopped. The reactor was allowed to cool down and depressurised before discharging its content. The nickel depleted reduction solution and powder thus obtained were separated by decantation. The spent solution was kept for AAS analysis to determine the residual nickel concentration and the powder was used as seeding material for the next densification. This process was repeated up to 5 densifications after which it becomes difficult to effectively suspend the dense nickel powder during reduction, leading to plastering on the reactor walls. At the end of the cycle (5 densifications) the powder was discharged from the autoclave, washed and dried in an oven at 80°C. The powder so obtained was weighed and characterized.

2.4. Instrumental analysis

Atomic absorption spectrometry (Thermo Scientific ICE 3000) was used in order to determine nickel concentration in the prepared solution for reduction and the resulting spent solutions. Laser diffraction technique was used for particle size distribution analysis. This was done with a Mastersizer 2000 equipped with a wet dispersion unit (Hydro 2000G) manufactured by Malvern instruments. This instrument is capable of measuring particle sizes from 0.02 to 2000

μm. In a typical analysis, the sample is prepared and introduced in the dispersion unit where it is dispersed to the correct concentration before being delivered to the optical bench. The purity of the original nickel powder and the one obtained after five densifications with different additive concentrations were determined by X-ray fluorescence analysis (XRF). This analysis was done with a Rigaku ZSX Primus II equipped with a rhodium target at 50 kV and 40 mA. Sample preparation consisted of making the powder into pellets by means of a hydraulic press. X-ray diffraction was used to identify the crystalline phases present in the nickel powder before and after reduction at different additive levels. The instrument used for this purpose was a Rigaku Ultima IV equipped with a copper target. The voltage and current at which the diffractometer was operated were 40 kV and 30 mA respectively. Spectra were acquired in the range of 2θ from 10° to 90° with a step size of 0.01° at the scanning speed of 1°/min. Scanning electron microscopy was performed in order to visualize the surface morphology and the structure of particles and agglomerates in the nickel powder samples. It was done using a TESCAN microscope coupled with an energy dispersive X-ray spectrometer (EDX). The information on surface area and porosity of the nickel powder was obtained by means of physisorption with nitrogen gas using Micromeritics TriStar 3000. Degassing was done at 90°C overnight with nitrogen gas.

3. Results and discussion

3.1. Volume distribution

Fig. 1 shows the volume based particle size distribution of nickel powder obtained after five densifications in the absence and presence of calcium lignosulphonate. It can be observed that the volume distributions were all bimodal. Comparing the peaks in the size range 13 – 182 μm of Fig. 1a, it can be seen that the peak area after five densifications in the absence of the additive is slightly higher than that of the seeds. As for the peaks at 182 – 955 μm the difference in area is hardly appreciable. However, there was a modal size shift from about 478 μm to 363 μm. This is an indication of particle breakage within that size region. These observations are reflected in the cumulative undersize distributions at 10%, 50% and 90% reported in Table 1.

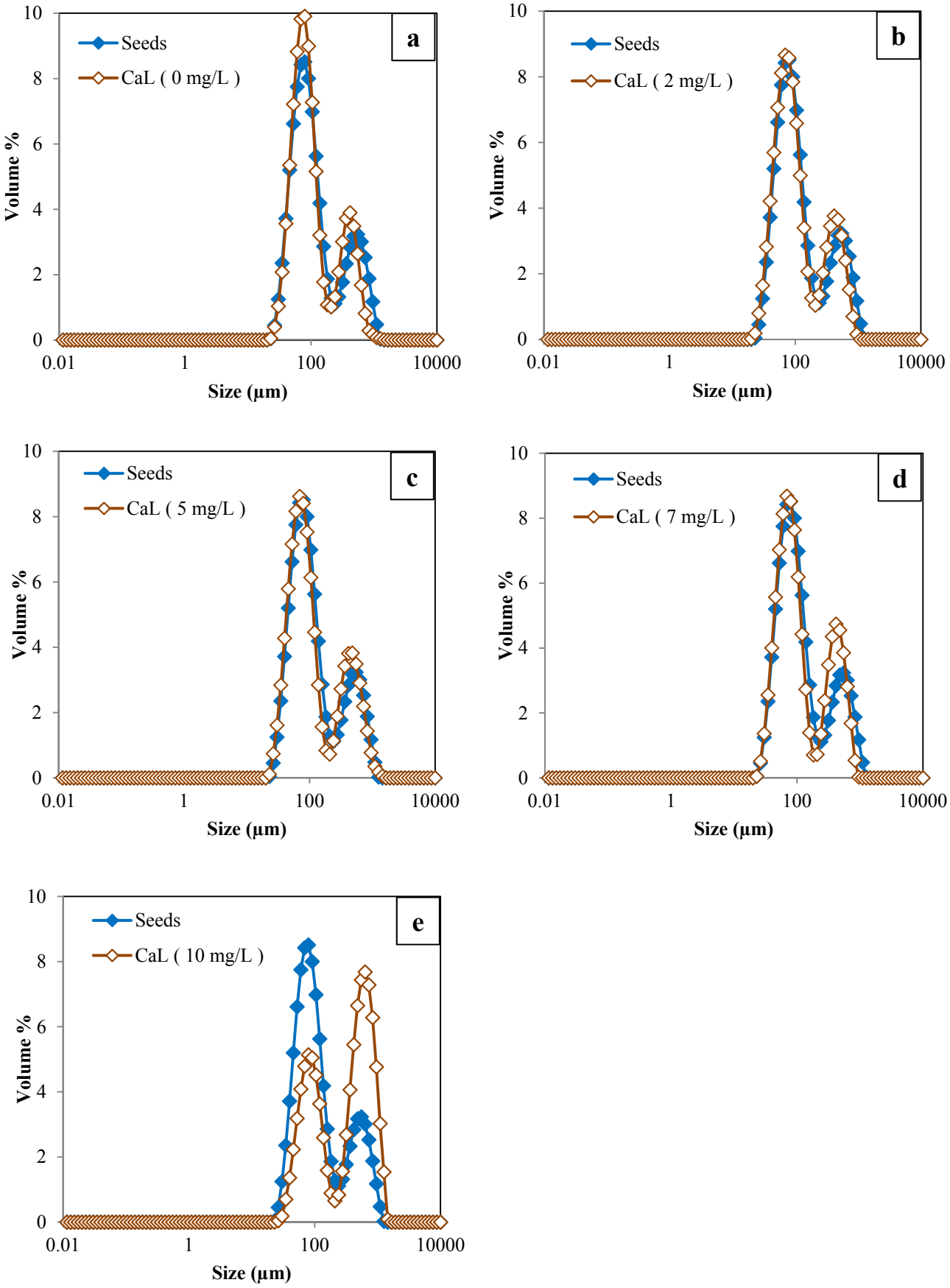

Fig. 1. Volume distributions in the absence and presence of CaL

A slight increase in the d (0,1) indicates size enlargement of seed particles in the smaller size fraction with subsequent densifications. This could be due to molecular growth, agglomeration or both. A sharp decrease in d (0,9) corresponds to a decrease in size in the larger size fraction. Furthermore, the slight decrease in d (0,5) suggests that larger particles were more affected than the smaller ones. This is consistent with the generally accepted view that breakage only affects larger particles or agglomerates larger than 100 µm (Schaer et al., 2001; Ntuli and Lewis, 2009).

Table 1

Volume distribution percentiles of the seed and powder obtained at the fifth densification with and without CaL

Powder	d(0,1) µm	d(0,5) µm	d(0,9) µm
Seed	42.399	87.488	528.436
CaL (0 mg/L)	43.133	81.482	405.324
CaL (2 mg/L)	40.161	82.431	442.220
CaL (5 mg/L)	40.269	82.654	504.417
CaL (7 mg/L)	41.501	84.521	462.440
CaL (10 mg/L)	56.901	365.261	820.288

The volume distributions of nickel powder in the presence of 2, 5 and 7 mg/L of calcium lignosulphonate are presented in Figs. 1b, 1c and 1d respectively. They all share common features namely a decrease in the modal size for the peaks at 182 – 955 µm, and a decrease in the cumulative undersize at 10%, 50% and 90% with respect to the seed. All these features indicate an increase in the proportion of smaller size particles. Based on the shape of the volume distributions, the shift in the modal size could be attributed to breakage. Breakage was more pronounced at 2 mg/L of calcium lignosulphonate followed by 7 and 5 mg/L as indicated by the d (0,9) values.

In contrast, the volume based particle size distribution of the powder obtained using 10 mg/L of calcium lignosulphonate (Fig. 1e) is unique compared to those obtained at lower concentrations. The area of the peak in the smaller particles region significantly dropped while

the opposite was observed in the larger particle size range. This corresponds to particle size enlargement. This is also reflected in the sharp increase in the cumulative undersize at 10, 50 and 90% as presented in Table 1. The overall increase in the particle size could be attributed to either agglomeration, molecular growth or both.

3.2. Number density distribution

This sub-section discusses the number distribution of the seed and nickel powder obtained at the fifth densification with the additive concentration varying from 0 to 10 mg/L. The number distributions were derived from the volume distributions as reported by Bodoza et al. (2013). Comparing the number distributions of the seed and that of the powder obtained in the absence of the additive, no significant change is observed as depicted in Fig. 2a. One would expect a decrease in the modal size and an increase in the peak area since breakage was identified as the main particulate process in the volume distribution analysis. The observed behaviour suggests that the effect of breakage was most likely damped by another parallel particulate process: agglomeration.

On the other hand at additive concentration of 2, 5 and 7 mg/L, the number distribution of the powder obtained after 5 densifications (Figs. 2b, 2c, 2d) shows an increase in the area under the curve with respect to the seed. This indicates an increase in particle number most probably as a result of breakage as suggested by the volume distributions.

At 10 mg/L of calcium lignosulphonate a shift in the modal size to the right and a decrease in the number distribution area are observed (Fig. 2e). The increase in the modal size corresponds to particle size enlargement. Findings which agree well with the volume distribution discussed earlier. The decrease in peak area signals an overall drop in the number of particles which can only be possible through agglomeration. However, an investigation conducted by Kunda et al. (1965) with the same additive in the concentration range 0.2 – 0.5 g/L for the ammonium carbonate system showed no evidence of agglomeration.

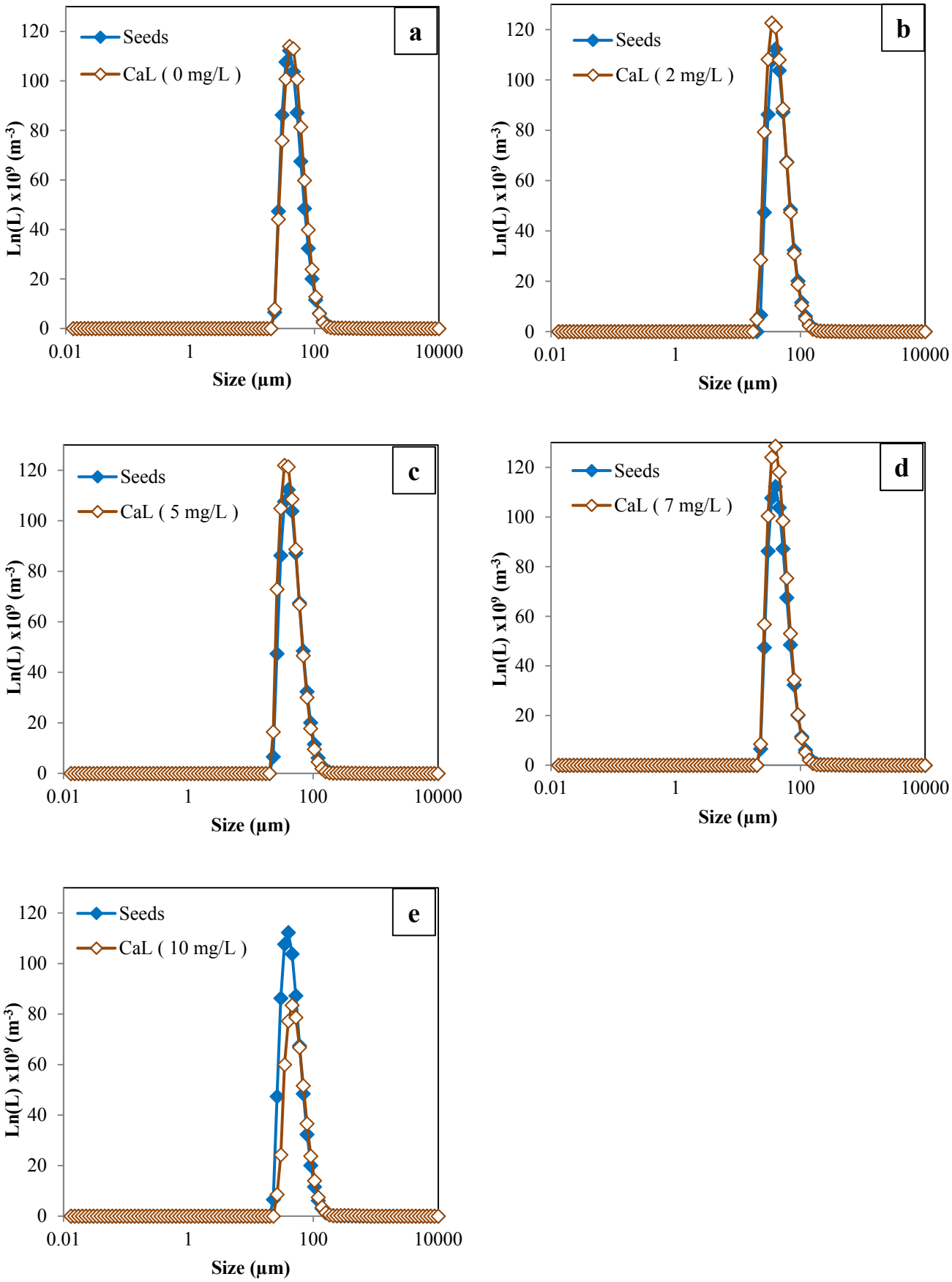

Fig. 2. Number distributions in the absence and presence of CaL

In all the cases, there was no significant shift in the modal size of the number distribution suggesting that breakage by attrition rather than fragmentation was the dominant breakage mechanism (Fig. 2). Fragmentation results in the breakage of particles into a number of particle fragment significantly altering the modal size of the seed particles.

3.3. Zeroth moment

The zeroth moment of the seed and nickel powder obtained after five densifications with different concentrations of calcium lignosulphonate is shown in Fig. 3. The zeroth moment is equivalent to the particle number in a given sample. This was calculated by the method used by Ntuli and Lewis (2009). The number of particles slightly increases at additive concentrations of 0, 2, 5 and 7 mg/L and significantly decreases at 10 mg/L. There was no significant difference in particle number at 2, 5 and 7 mg/L of additive. However, these three additive dosages resulted in the highest particle number. The particle number increase is normally due to either breakage or nucleation. A nucleating system is generally characterized by fines generation which significantly change the modal size of the number distribution and the d (0,1). Since none of these characteristics were observed, nucleation was ruled out. In addition, the fact that there was no modal size shift is an indication that breakage occurred by attrition rather than by fragmentation. The decrease in particle number is attributed to agglomeration as discussed earlier.

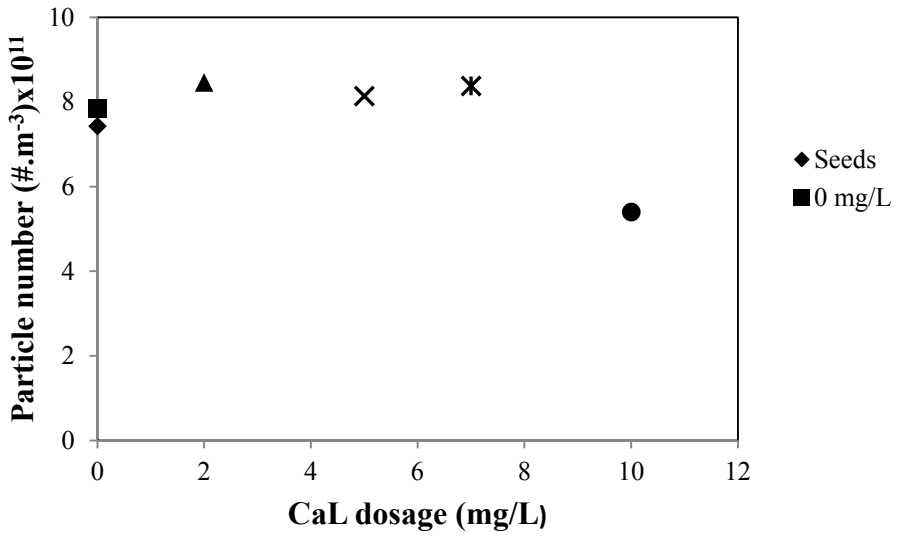

Fig. 3. Particle number at different concentrations of CaL

3.4. Second moment

The second moment which is equivalent to the particle external surface area was derived from the transformation of the volume based particle size distribution as reported in the work of Ntuli and Lewis (2009). The results for the second moment at different concentrations of calcium lignosulphonate are reported in Fig. 4. An examination of Fig. 4 shows that the external surface area of the powder particles was not significantly affected after five densifications regardless of the additive concentration. One would expect a higher surface area from 0 to 7 mg/L of additive due to the extent of breakage in the specified dosage range and a lower surface area at 10 mg/L of additive since agglomeration was more dominant. While the first expectation was observed, the second was not. Thus agglomeration was found to have little effect on the external surface area compared to the particle number.

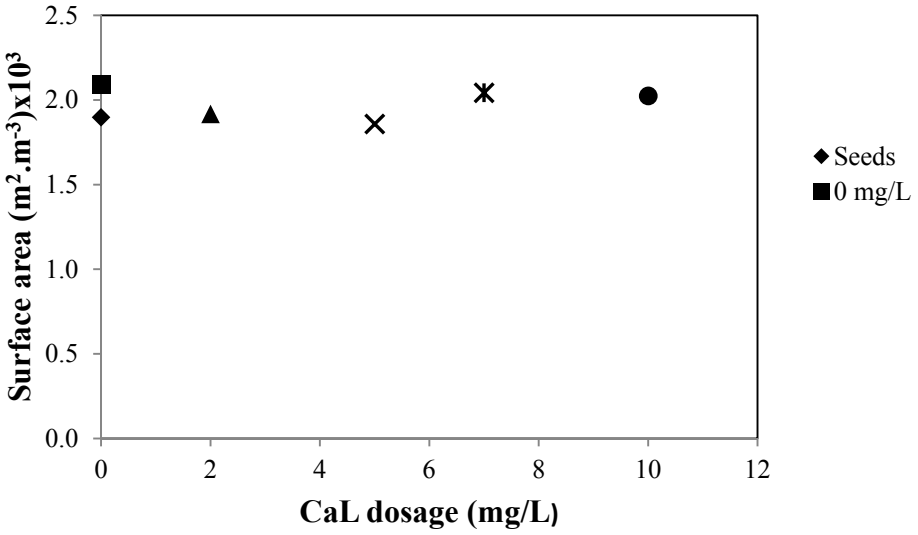

Fig. 4. Particle surface area at different concentrations of CaL

3.5. Number and volume based mean particles sizes

The number based mean size $\overline{L}_{1,0}$ which represents what happens to the smaller size particles of the PSD is shown in Fig. 5a. No significant difference in the $\overline{L}_{1,0}$ was observed in the absence of the additive with respect to the seed. In the presence of the additive the $\overline{L}_{1,0}$ decreased and steadily increased with increasing additive dosage. The number based mean size of the powder obtained at 2, 5 and 7 mg/L of additive was lower than that of the seed while the opposite was true at 10 mg/L. These findings suggest that calcium lignosulphonate acted as a growth promoter. In fact, a growth promoter also promotes agglomeration since agglomeration involves particle collision and cementing of particles by growth of a metallic bridge. However, its growth promotion ability becomes apparent at a concentration of 10 mg/L. It can be proposed that the strength of the agglomerate bonds is weaker at lower concentrations.

As opposed to the number mean, the mass moment mean size shows what happens to the larger size particles of the PSD. Fig. 5b shows the mass moment mean size D (4, 3) for the seed and the powder obtained with the additive concentration from 0 to 10 mg/L. There was a relative decrease in the D (4, 3) of the powder at additive concentration range 0 – 7 mg/L. The highest D (4, 3) was obtained when the additive concentration was raised to 10 mg/L. A relatively lower value in the D (4, 3) indicates breakage while a higher value is a sign of agglomeration. Based on the observed trend it could therefore be concluded that the extent of breakage was suppressed by increasing additive dosage which then promoted agglomeration.

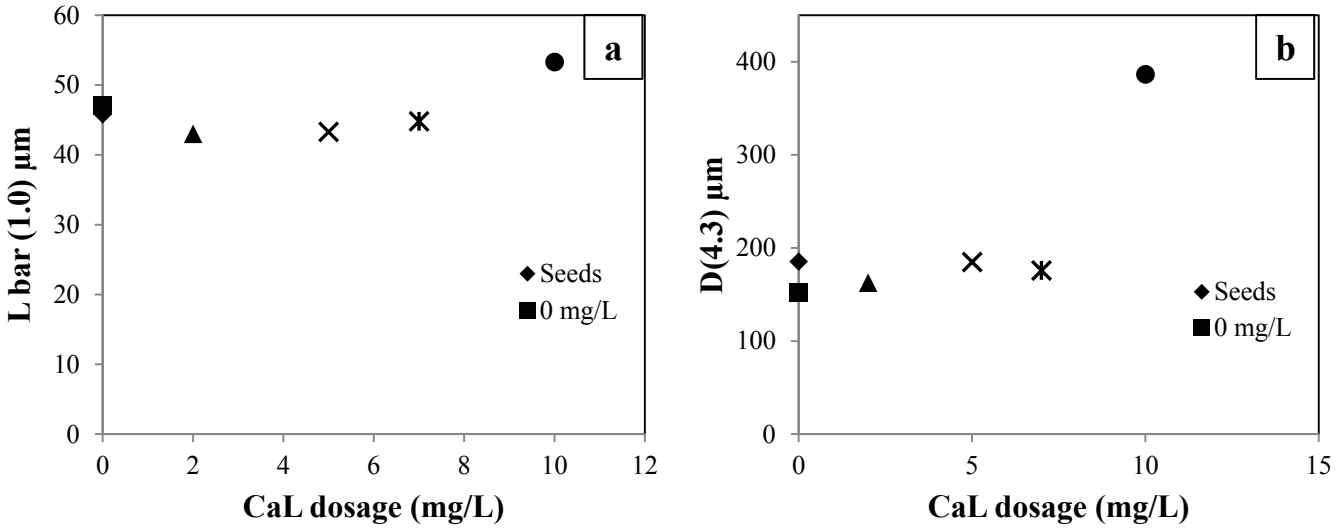

Fig. 5. Number and volume based mean particle sizes at different CaL dosages

3.6. Third moment

The third moment which is equivalent to particle volume is shown in Fig. 6. It was calculated based on the liquor mass balance. There was an increase in particle volume with respect to the seed in the presence and absence of the additive. However, the particle volume was comparable for the entire additive concentration range (0 – 10 mg/L). It could be argued that growth was responsible for the particle volume increase since nucleation was ruled out.

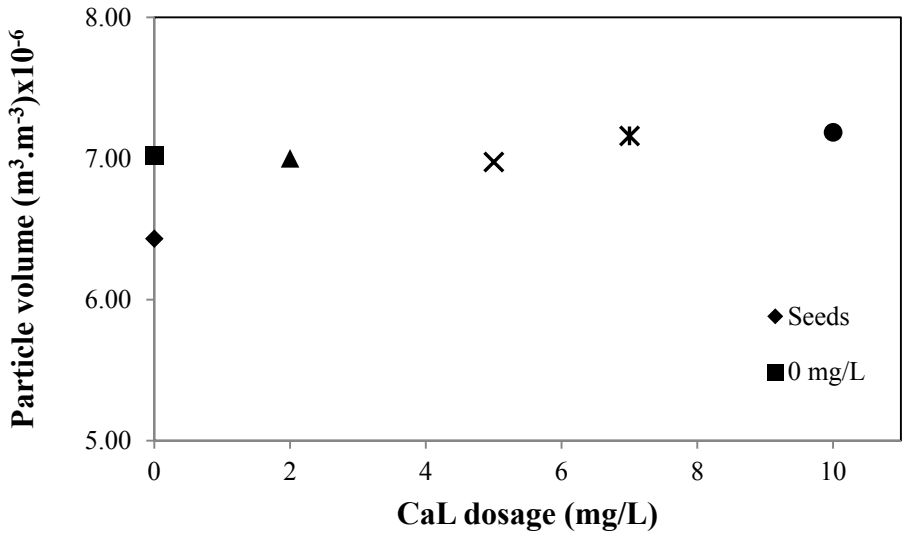

Fig. 6. Third moment at different CaL dosages

3.7. Specific surface area and reduction rate

There was a significant overall decrease in the specific surface area of the powder obtained with subsequent densifications in the absence and presence of calcium lignosulphonate as shown in Fig. 7a. Comparing this data with the second moment it becomes evident that the changes in the specific surface area were more likely caused by changes in the pore size rather than the external surface area. This hypothesis is consistent with the comparison of Fig. 7a and 7b which shows an inverse relationship between the BET surface area and the pore size of the powder. Overall, the highest specific surface area was observed at a CaL dosage of 10 mg/L, which was significantly higher than that at lower concentrations. This indicates that at higher concentrations (>10 mg/L) CaL increases powder porosity.

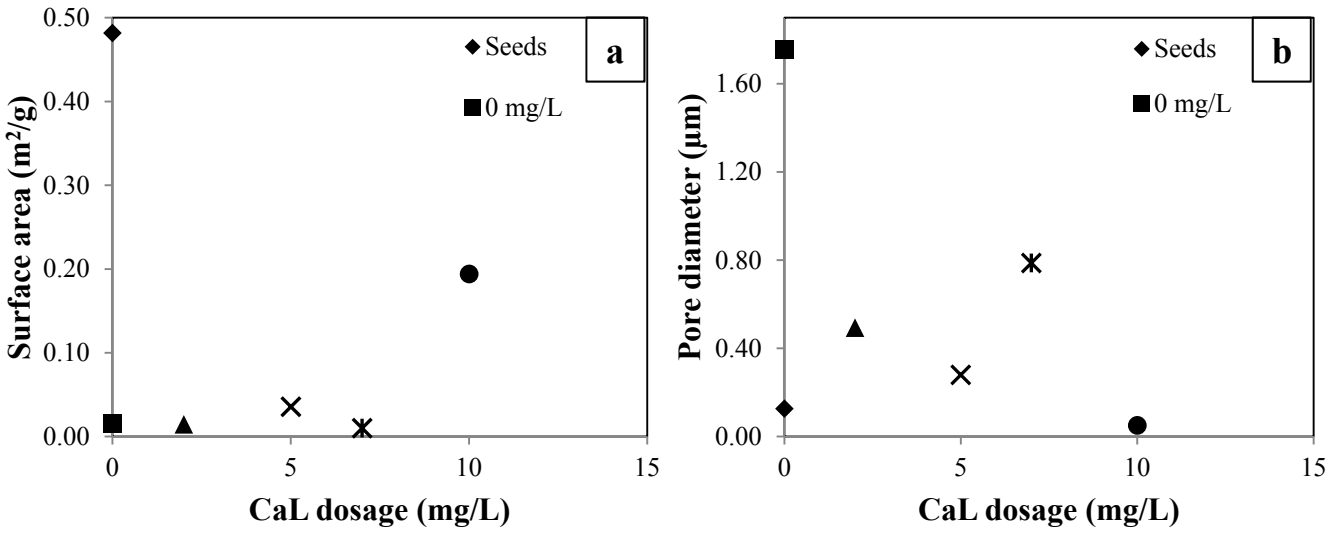

Fig. 7. Specific surface area and pore diameter at different CaL dosages

Nickel depletion rate during the reduction process was studied in the absence and presence of calcium lignosulphonate. However, the effect of the additive was investigated only at 7 and 10 mg/L dosages since major changes based on the PSD evolution were observed within that concentration range. Fig. 8a depicts the reduction rate as a function of densifications and the additive dosage. It can be observed that, in general, the reduction rate decreased with subsequent densifications regardless of the additive concentration. Fig. 8b shows the reduction rate averaged over the five densifications in each cycle with different additive dosage. The average reduction rate increased as the additive dosage was raised from 7 to 10 mg/L. These findings are in accord with the above discussed surface areas since the reduction rate has been reported (Needes and Burkin, 1975) to be proportional to the seed surface area. The increase in the average reduction rate in the presence of calcium lignosulphonate is an indication that this additive acted as a growth promoter.

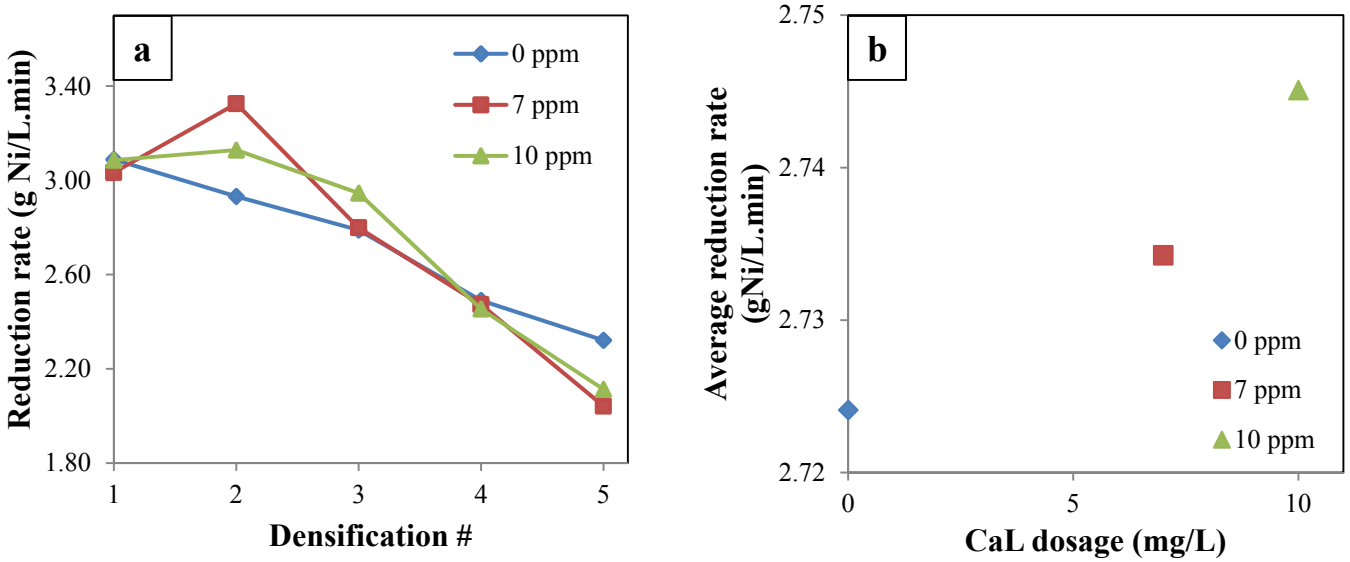

Fig. 8. Reduction rate as a function of densification (A) and CaL dosage (B)

3.8. Powder purity and morphology

Table 2 shows the composition of nickel seed and powder obtained in the presence and absence of calcium lignosulphonate for selected elements. The reported values are in weight percentage. No significant difference could be observed in terms of nickel content of the powder obtained with different additive dosage relative to the seed. There was no trend in the sulphur content of the powder. The lowest and highest sulphur content were observed at 7 and 10 mg/L of additive respectively. However, the amount of calcium in the powder was found to increase with increasing additive dosage except for 0, 2 and 7 mg/L which showed no traces of it. Since the seed initially contained calcium one can argue that in these cases the amount of calcium was below the detection limit of the instrument.

Table 2

Nickel powder composition for selected elements

Powder	%Ni	%S	%Ca
Seed	98.9	0.165	0.0127
CaL (0 mg/L)	98.1	0.110	BDL
CaL (2 mg/L)	99.0	0.347	BDL
CaL (5 mg/L)	98.9	0.083	0.0160
CaL (7 mg/L)	99.2	0.080	BDL
CaL (10 mg/L)	98.5	0.619	0.0258

BDL = Below detection limit

The powder morphology was studied by means of SEM micrographs at a magnification of 300 as shown in Fig. 9. It can be clearly seen that there was an overall increase in the particle size with subsequent densifications in the absence and presence of calcium lignosulphonate. The micrographs suggest that breakage and agglomeration occurred during reduction at varying degrees. The near spherical particles appear to have been formed from the agglomeration of smaller particles resulting in a powder of a closed nature. No significant difference could be observed in terms of the final powder morphology expected with and without calcium lignosulphonate after five densifications. However, the particles were more well-defined and larger with increasing additive concentrations above 2 mg/L. This can be attributed to the fact that the powder is still in its formative stage as it normally takes 10 – 15 densifications for the powder to develop into its final defined shape, as previously observed from industrial studies (Ntuli and Lewis, 2009).

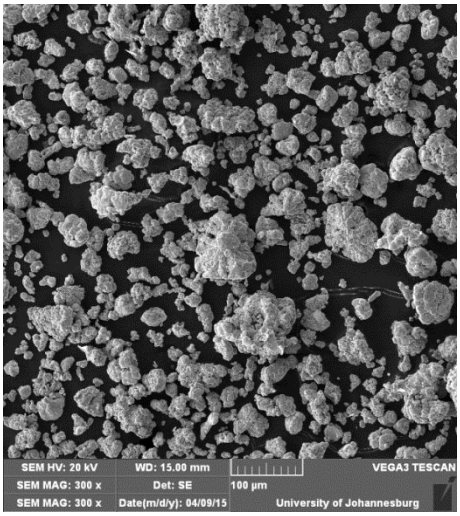

Seed

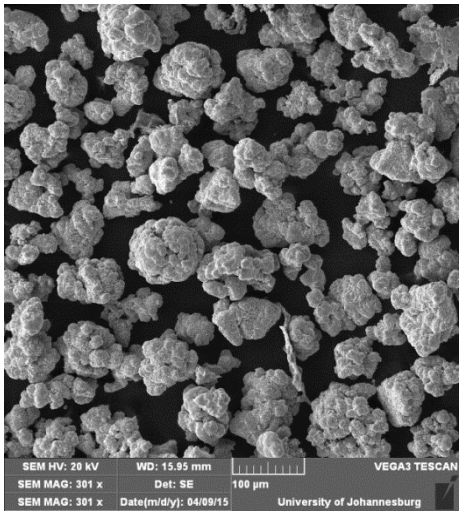

0 mg/L

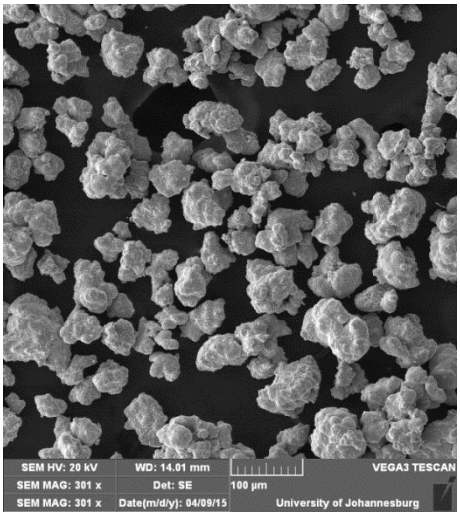

2 mg/L

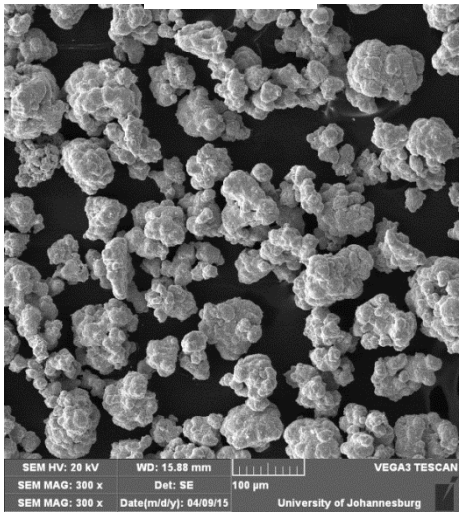

5 mg/L

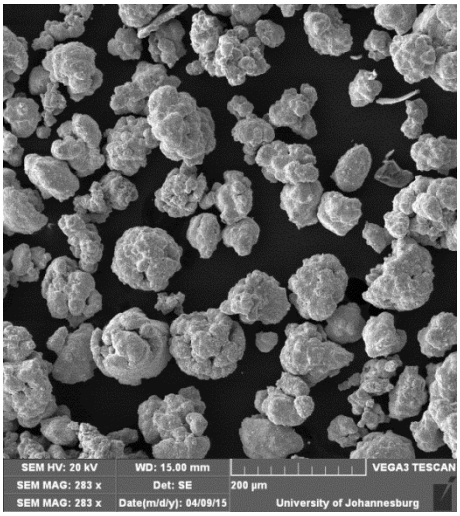

7 mg/L

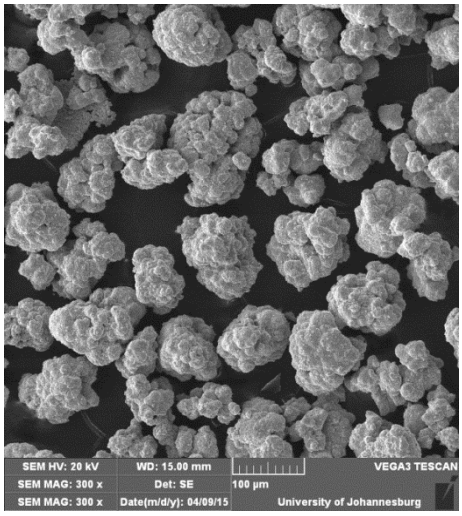

10 mg/L

Fig. 9. SEM micrographs at different CaL dosages

3.9. X-ray diffraction

Fig. 10 shows the X-ray diffraction pattern of the nickel powder. Since there was no difference in the diffraction patterns of the powder obtained in the presence and absence of both additives, only one diffractogram is presented. The peaks are assigned, from left to right, to the 111, 200 and 220 planes of face centered cubic nickel. No other phases were detected in all of the samples.

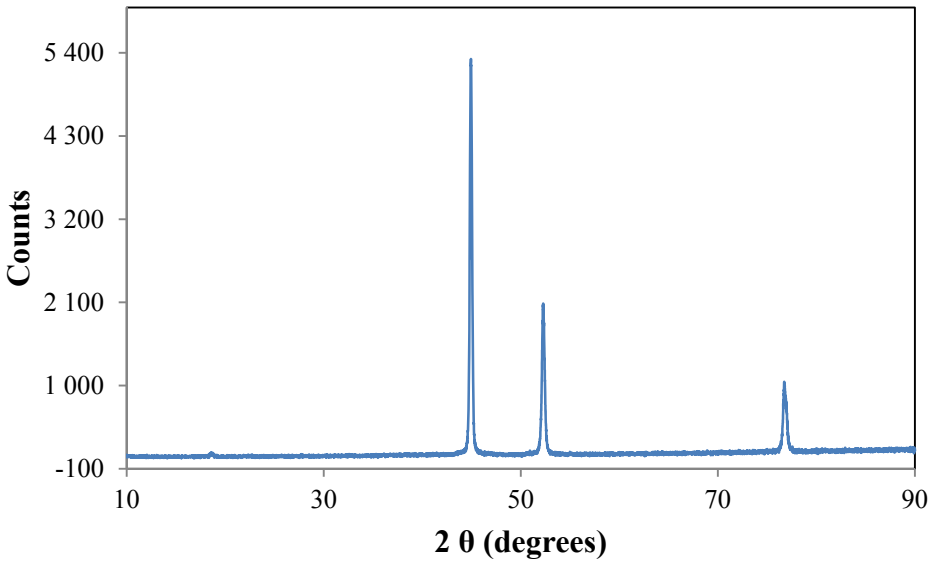

Fig. 10. Nickel powder diffractogram

4. Conclusions

Calcium lignosulphonate was investigated as an additive in the hydrogen reduction of nickel ammine sulphate solutions. Calcium lignosulphonate was found to promote growth. This growth promoting effect became more evident when the additive concentration was raised to 10 mg/L. Since a growth promoter also promotes agglomeration, there was a significant drop in particle number at this additive concentration. The system was dominated by breakage when calcium lignosulphonate was used at lower concentrations. These findings were supported by SEM images which show relatively larger particles at 10 mg/L. X-ray fluorescence data shows that there was no significant difference in terms of nickel content of the powder obtained in the presence and absence of calcium lignosulphonate. However, it is noted that the powder obtained at a concentration 10 mg/L had the highest sulfur content. The reduction rate was

found to increase as calcium lignosulphonate concentration was increased from 7 to 10 mg/L. This is an indication that this additive acted as a reduction catalyst. The increase in the reduction rate could be attributed to a change in the pore area since no remarkable difference could be observed in the external surface area. The X-ray diffraction pattern of the nickel powder was identical at all additive concentrations. The only identifiable peaks were that of the face centered cubic nickel phase.

References

Agrawal, A., Kumar, V., Pandey, B.D., Sahu, K.K., 2006. A comprehensive review on the hydro metallurgical process for the production of nickel and copper powders by hydrogen reduction. Mater. Res. Bull. 41**,** 879-892.

Bodoza, T.F., Ntuli, F., Chauke, D.F., Muzenda, E., 2013. The effect of poly(ethylene-alt-maleic anhydride) on the reduction crystallisation behaviour of nickel powder. Can. J. Chem. Eng. 91**,** 822-829.

Chou, E.C., Crnojevich, R.P., Koehler, H., 1976. Catalytic hydrogen reduction of metals from solutions. US Patent 3,989,509.

Crundwell, F.K., Moats, M.S., Ramachandran, V., Robinson, T.G., Davenport, W.G., 2011. Hydrogen reduction of nickel from ammonical sulfate solutions. In: Crundwell, F.K., Moats, M.S., Ramachandran, V., Robinson, T.G., Davenport, W.G. (eds.), Extractive Metallurgy of Nickel, Cobalt and Platinum Group Metals. Elsevier, Oxford, pp. 347-354.

Evans, D.J.I., 1968. Production of metals by gaseous reduction from solution - Processes and chemistry. In Advances in Extractive Metallurgy. The Institution of Mining and Metallurgy, London, pp. 831-907.

Habashi, F., 1999. A textbook of hydrometallurgy. Métallurgie Extractive Québec.

Kunda, W., Evans, D.J.I., 1968. Controlling the properties of nickel powders produced by the hydrogen reduction of nickel ammine sulphate solutions. Proceedings of the 2nd European Symposium on Powder Metallurgy. Germany, pp. 1-25.

Kunda, W., Evans, D.J.I., Mackiw, V.N., 1965. Effect of addition agents on the properties of nickel powders produced by hydrogen reduction. Proceedings of the International Powder Metallurgy Conference. New York, pp. 1-33.

Luidold, S., Antrekowitsch, H., 2007. Hydrogen as a reducing agent: State-of-the-art science and technology. JOM. 59**,** 20-26.

Meddings, B., Mackiw, V.N., 1965. The gaseous reduction of metals from aqueous solutions.

Naboychenko, S.S., Murashova, I.B., Neikov, O.D., 2009. Production of Nickel and Nickel-Alloy Powders. In: Neikov, O.D., Naboychenko, S.S., Murashova, I.V., Gopienko, V.G., Frishberg, I.V., Lotsko, D.V. (eds.), Handbook of Non-Ferrous Metal Powders. Elsevier, Oxford, pp. 369-398.

Needes, C.R.S., Burkin, A.R., 1975. Kinetics of reduction of nickel in aqueous ammoniacal ammonium sulphate solutions by hydrogen. In: Burkin, A.R. (ed.), Leaching and reduction in hydrometallurgy. The Institution of Mining and Metallurgy, London, pp. 91-96.

Ntuli, F., Lewis, A.E., 2007. The influence of iron on the precipitation behaviour of nickel powder. Chem. Eng. Sci. 62**,** 3756-3766.

Ntuli, F., Lewis, A.E., 2009. Kinetic modelling of nickel powder precipitation by high-pressure hydrogen reduction. Chem. Eng. Sci. 64**,** 2202-2215.

Osseo-Asare, K., 2003. Hydrogen reduction of metal Ions: An electrochemical model. Electrometallurgy and Environmental Hydrometallurgy. pp. 1151-1165.

Saarinen, T., Lindfors, L.E., Fugleberg, S., 1998. A review of the precipitation of nickel from salt solutions by hydrogen reduction. Hydrometallurgy 47**,** 309-324.

Schaer, E., Ravetti, R., Plasari, E., 2001. Study of silica particle aggregation in a batch agitated vessel. Chem. Eng. Process. 40**,** 277-293.